Available online at www.sciencedirect.com
ScienceDirect
Trans. Nonferrous Met. Soc. China 33(2023) 3222−3234
Transactions of Nonferrous Metals Society of China
www.tnmsc.cn

# Pollution characteristics and ecological risk apportionment at a smelting site based on stochastic simulation

Xing-hua LUO[1], Jia-qing ZENG[1], Chuan WU[1], Kun-yan QIU[2], Chao-ran LI[2], Wen-shun KE[1], Sheng-guo XUE[1]

1. School of Metallurgy and Environment, Central South University, Changsha 410083, China;
2. National & Local Joint Engineering Research Center for Applied Technology of Hybrid Nanomaterials, Henan University, Kaifeng 475004, China

Received 8 May 2022; accepted 9 September 2022

**Abstract:** Geostatistical analysis and Pb isotope tracing were used to characterize the distribution patterns and the sources of heavy metals at a lead smelting site. Furthermore, ecological risks were apportioned based on stochastic theory. The results showed that soils were seriously contaminated by Pb, Zn, As, Cd, Cr and Hg, which reflected strong spatial heterogeneity. Based on MixSIAR model, the density distributions of three endmembers were deconstructed, in which 49.9% of Pb came from smelting activities, and 16.4% and 33.7% from coal combustion and geological source, respectively. Along with the integration of the apportionment of Pb isotope and Monte Carlo simulation, concentration-oriented probabilistic risk indicated that the moderate risk level was dominant, and Cd, As, Pb and Hg were sensitive factors. Source-oriented probabilistic risk presented that smelting contributed the most to risk accumulation. Therefore, the control of Cd, As, Pb and Hg and the disposal of potential smelting sources should be in priority.

**Key words:** smelting sites; heavy metals; Pb isotope; stochastic simulation; ecological risk

## 1 Introduction

Smelting activities have aggravated the accumulation of heavy metals in soils [1,2], which not only damages the soil ecosystem, affects the redevelopment of lands, but also threatens human health and ecological security [3−5]. Additionally, heavy metals could pass through eluviation, leaching and osmosis into groundwater, thereby creating further challenges to water quality and sustainable water supply [6,7].

Previous studies have been focused on pollution evaluation, risk assessment and source identification of heavy metals in soils [8−10]. High levels of mobile fractions of Cd and Zn were determined in the soils surrounding a typical Pb/Zn smelter, posing great ecological risks [11]. JIANG et al [12] reviewed the heavy metals in soils around different nonferrous smelteries (Cd, 19.8 mg/kg; Cu, 265 mg/kg; Pb, 1536 mg/kg; Zn, 1371 mg/kg) and illustrated that Cd and Pb were the major contributors to the health risks. Smelting has become the primary industry responsible for the pollution by releasing large amounts of heavy metals into soil in China [10]. However, current distribution patterns and source identification of heavy metal pollution were concentrated more on investigations in regions surrounding the industrial sites [13,14]. The occurrence and characteristics of contaminants at typical sites scale are hitherto poorly understood, with limited reference significance for effective pollution prevention and control. In addition, spatial variations and source randomness of heavy metals are exhibited in contaminated sites [15], resulting in the uncertainty

**Corresponding author:** Sheng-guo XUE, Tel: +86-13787148441, E-mail: sgxue@csu.edu.cn
DOI: 10.1016/S1003-6326(23)66329-0

of pollution evaluation. Geostatistical methods could well fit pollution distribution and are widely used to describe the pollution characteristics [1]. The provenance of heavy metals and contribution of different endmembers to smelting-affected soils have been conducted by multivariate statistical methods, such as positive definite matrix factor analysis (PMF), principal component analysis (PCA) and UNMIX model [9,15]. Such statistical analysis requires large datasets and can hardly yield reliable quantitative results [16]. Due to the stability in physical and chemical processes, Pb isotopes have been successfully used in source identification at present [9]. For example, Pb binary isotope mixing model identified that heavy metal accumulation in soils represented the legacy of former Pb/Zn smelting [17]. Isotopic signatures of Pb from different sources may also have potential ambiguities [15]. However, binary linear models always quantify in a deterministic manner, and the reliability of the results is poor. Meanwhile, binary linear models face inadequacies in calculating the apportionment of multiple anthropogenic sources [15]. The MixSIAR model has been used to trace more than three endmembers and convincing results have been obtained in quantifying Pb isotope sources [18]. In addition, the MixSIAR model considers the uncertainty of the provenance contribution, which weakens the limitations of isotopic ratio analysis and can more accurately identify the contribution rates of different endmembers.

From the perspective of the biological toxicity of heavy metals, Hakanson ecological hazard index (RI) integrates the current concentration and toxicity of each heavy metal to comprehensively evaluate the pollution level [14,19]. Most parameters adopted in existing empirical models of ecological risk assessment are deterministic, which mainly rely on the total heavy metal concentrations and specific toxic coefficients [20]. However, there exist some inherent issues such as the randomness of concentrations and the subjective selection of toxicity response coefficient [21]. These important issues have been underestimated in previous studies. In particular, heavy metals presented extreme spatial variability in smelting sites [1]. It is tough to utilize conservative point estimation methods with deterministic parameters to estimate ecological risk accurately and diagnose the most sensitive factor. Fortunately, Monte Carlo simulation could define the probability of exceeding the guide threshold with few data and recognize sensitive factors of risk control [19,21]. The introduction of Monte Carlo simulation for probabilistic risk assessment is more accurate due to its ability to minimize uncertainty and variability effectively. Additionally, previous risk assessments were prone to be concentration-oriented [22], failing to differentiate the risk burden between natural sources and anthropogenic activities. Spatial variation in heavy metals caused by different sources ultimately contributes differentially to ecological risks [20]. Given the uncontrollability of naturally occurring heavy metals, our primary focus is on clarifying source-oriented pollution responsibilities. However, so far, the risk evaluation of heavy metals in soils is focused on conservative point estimation methods with deterministic parameters. Few reports consider the uncertainty of pollution evaluation caused by spatial variation and source randomness.

The main goals in present study were: (1) to analyze the distribution patterns of heavy metals via geostatistical methods; (2) to explore the provenance of heavy metals in soils and quantify the contribution of each end-member, and (3) to evaluate the concentration/source-oriented ecological risks caused by heavy metals and diagnose the sensitive factors using a probabilistic approach.

## 2 Experimental

### 2.1 Site description

The abandoned Pb smelting site is in the Henan province, central part of China (112°26′15″E, and 35°10′39″N). This region belongs to an ecological tourism area with scenic natural landscapes, which is characterized by valley-like topography running from northwest to southeast. It has a climate of temperate monsoon with the temperature of 14.4 °C and annual rainfall of 568 mm on average. The soils can be divided into loam, sandy loam and clay. The study area is poor in groundwater resources with deep groundwater levels (>7.0 m). The smelter was put into operation in 1996 with a Pb production of 22 kt/a and was permanently shut down in 2012. A preliminary background review and site survey revealed that there were no complete covering barriers in major

production areas. The remaining slags and raw materials were disposed directly on the ground and apparent contamination leaks occurred at the site.

### 2.2 Sampling and chemical analysis

The crawler probe (JDL150) was used to drill subsurface soil cores. Sampling points were reasonably established at major smelting sections, including raw material warehouse (A), electrolysis section (B), waste dumps (C), wastewater treatment area (D), furnace area (E) and coal storage area (F) (Fig. 1). The sampling depth of each point reached the weathered rock and sampling was conducted under the technical guidelines for monitoring during risk control and remediation of soil contamination of land for construction (HJ 25.2—2019). The upper 3.0 m layer was sampled every 0.5 m, and the lower 3.0−5.0 m layers was sampled every 1.0 m. Basic information including the soil type was recorded in detail. The field records showed that the layer was almost entirely backfilled soils with complex properties from top to base (0−5.0 m). Moreover, soil sampling not only included the typical functional regions but also covered the surface soil (0−0.5 m, Fig. 1) of the whole site and would provide representative samples to evaluate heavy metal contamination status. All samples were stored in polyethylene bags and brought back to the laboratory.

Soil samples were air-dried and sieved through a 2 mm mesh sieve before chemical analysis. For determination of the heavy metal concentration, approximately 0.2 g soils were digested using a microwave with a ternary acid mixture ($HNO_3$/HCl/HF, 3:1:1, volume ratio). The digestion liquids were filtered and diluted with distilled water to a suitable concentration for analysis. Total concentrations of As, Cd, Cr, Cu, Pb, Zn, Hg, Ni, Pb and Zn were determined using inductively coupled plasma-optical emission spectroscopy (ICP-OES, ICAP 7000 Series, Thermo Scientific, USA) [6,23]. Quality control and assurance were conducted by preparing reagent blanks, duplicates and a certified reference material (GBW07404) as the same procedures. High accuracy was shown and recovery rates ranged from 89% to 112%.

### 2.3 Pb isotope analysis

The three deepest soil cores (5.0 m, the mean concentration of Pb was 55.8 mg/kg) were uncontaminated and identified as soil background. The digestion procedures for analyzing Pb isotopes were the same as described for the metal concentration. Conventional anion exchange techniques (200−400 mesh AG1-X8 resin) with dilute HBr were used to separate and purify the Pb in digestion samples. Pb isotopes were estimated by multi-collector inductively-coupled plasma-mass spectrometry (Neptune MC-ICP-MS, Thermo Fisher Scientific, USA) at the State Key Laboratory of Ore Deposit Geochemistry, Guiyang, China. The results were expressed as ratios of $^{208}Pb/^{204}Pb$, $^{207}Pb/^{204}Pb$ and $^{206}Pb/^{204}Pb$. To compensate for any mass bias and assess precision, replicate analysis of certified reference material NIST SRM 981 were run after every batch of 5 samples. All replicated results (Table S1 in Supplementary data (SD)) were consistent with the reference value [17], which was in line with Pb isotope test accuracy requirements. By matching the Pb isotopic compositions of the

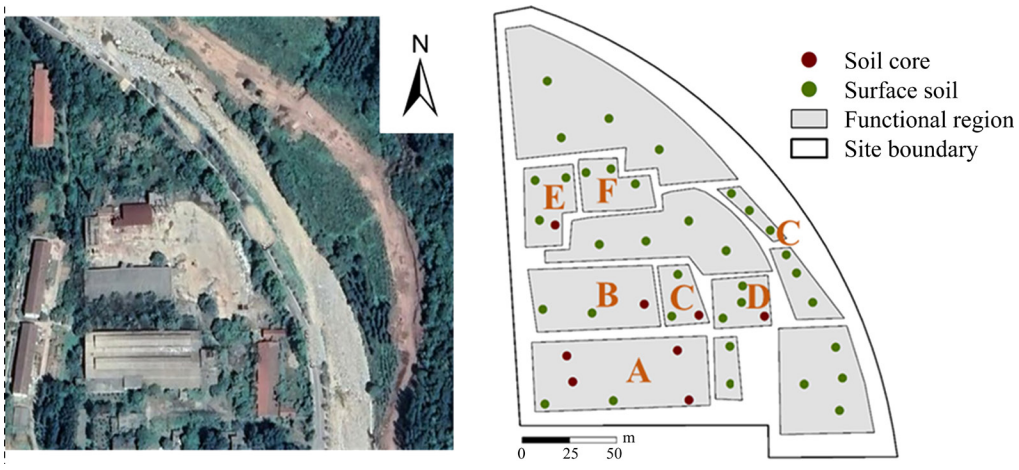


**Fig. 1** Locations of sampling and functional regions at smelting site

contaminated soils with those of potential sources, major sources of the Pb in the site can be identified and quantified [9]. The contributions of potential Pb sources were calculated using the MixSIAR model, which is based on Bayesian analysis and explicitly accounts for uncertainties in isotope values [24].

### 2.4 Ecological risk assessment for heavy metal contamination

The Hakanson ecological hazard index method was applied to assessing the metal pollution status of the abandoned site using the risk intervention value (GB 36600 — 2018), the superfund soil screening guidance of the United States [1]. The index was calculated as

$$C_{\mathrm{f}}^{i}=\frac{C^{i}}{C_{\mathrm{n}}^{i}} \tag{1}$$

$$E_{\mathrm{r}}^{i}=C_{\mathrm{f}}^{i}\cdot T_{\mathrm{r}}^{i} \tag{2}$$

$$\mathrm{RI}=\sum_{i=1}^{m}E_{\mathrm{r}}^{i} \tag{3}$$

where $C_{\mathrm{f}}^{i}$ is the single pollution index of $i$ heavy metal. $C_{\mathrm{n}}^{i}$ and $C^{i}$ are sample concentrations and reference values of $i$ heavy metal, respectively. $E_{\mathrm{r}}^{i}$ is the potential ecological risk factor for a given element; $T_{\mathrm{r}}^{i}$ is the toxic-response factor of $i$ heavy metal and this value for As, Cd, Cr, Cu, Hg, Ni, Pb and Zn is demonstrated to be 10, 30, 2, 5, 40, 5, 5 and 1, respectively. RI is the requested potential ecological risk index and different classifications are delineated in Table S2 of SD.

In addition, the density distribution of potential endmembers, resolved by MixSIAR model, was adopted to quantify the contribution of different sources to ecological risks. Through multiplying the risk values of heavy metals by the apportioned rates of the identified sources, the source-oriented ecological risks were then obtained [19]. The values of metal concentrations were simulated by Monte Carlo model to minimize the uncertainties associated with the risk calculation [21], as recommended by USEPA. The simulation ran for 50000 iterations (Monte Carlo sampling method with the confidence of 95%) and was then used for assessing ecological risk. To characterize the contribution of each heavy metal on ecological hazard index, a sensitivity analysis function was used [19].

### 2.5 Statistical analysis

Inverse distance weighted interpolation (IDW) was performed in ArcGIS 10.2 to evaluate the distribution characteristics of heavy metals at the site scale. Origin Pro 2021 was used for data fitting and image processing on the vertical distribution of heavy metals. Pearson correlation analysis was conducted to explore the correlations among different heavy metals. MixSIAR is a package in R (version 3.1.12) and was used to build source analysis model. The Monte Carlo simulation was conducted by Oracle Crystal Ball.

## 3 Results and discussion

### 3.1 Descriptive characteristics of heavy metal pollution in soils

Comprehensive surveys of soil heavy metals were conducted at the abandoned Pb smelting site. The risk intervention value (GB 36600—2018) and the superfund soil screening guidance of the United States were adopted as reference values in this study [1]. The descriptive statistics of heavy metals in soil cores and surface soils are presented in Table 1. Summary data of the soils showed that Pb, Zn, As and Cd in surface soils were commonly present at extremely high concentrations in the whole site. The mean contents of Pb, Zn, As and Cd were 19160, 10840, 1380 and 400 mg/kg, respectively. The mean and maximum levels exceeded the corresponding reference values several times, indicating serious pollution. Cd, Zn, Pb and As have been frequently reported as dominative pollutants due to intensive smelting activities [2,4]. The content of Cr also exceeded the reference value in some samples, with an average of 115 mg/kg. The Hg contamination level was slight in the whole smelter, with only several samples out of limits. Statistical results indicated that the concentrations of Ni and Cu were within the range of risk intervention value (GB 36600—2018). In general, soil cores showed lower levels of contamination than surface soils, and the mean values of Pb, Zn, As and Cd were 1965, 511, 631 and 61.9 mg/kg, respectively. The over-standard rate was as follows: As > Cr > Pb > Hg > Cd. Spatial variability is usually associated with the weathering of soil parent materials or external input [2]. High coefficient of variation (CV) values of most heavy metals (ranging from 40.5% to

196%) represented severe variability of heavy metals in the site, suggesting the large heterogeneity of extrinsic input [12,19].

### 3.2 Spatial distribution of heavy metals at site scale

To clarify the pollution characteristics of heavy metals more intuitively, the horizontal distribution of six heavy metals (out of limits) in surface soils was obtained by IDW interpolation analysis (Fig. 2). Significant heterogeneities were observed for all heavy metals from the perspective of horizontal spatial features. There were multiple hotspots for heavy metal pollution, including typical functional regions and the non-production areas. Despite the differences in the concentrations of Pb and Cd

**Table 1** Descriptive statistics of heavy metal concentration in soils (mg/kg)

| Site | Parameter | Pb | Zn | Cd | As | Cu | Ni | Hg | Cr |
|---|---|---|---|---|---|---|---|---|---|
| Surface soil ($n$=43) | Mean | 19160 | 10840 | 400 | 1380 | 3434 | 92.0 | 28.7 | 115 |
| | Min | 477 | 271 | 3.10 | 264 | 64.0 | 39.3 | 2.20 | 21.6 |
| | Max | 47342 | 35190 | 1661 | 2947 | 9380 | 234 | 124 | 255 |
| | CV/% | 71.1 | 99.6 | 107 | 59.9 | 78.4 | 40.5 | 117 | 43.4 |
| | OSR/% | 89.2 | 56.8 | 59.5 | 100 | 0 | 0 | 10.8 | 83.8 |
| Soil core ($n$=52) | Mean | 1965 | 511 | 61.9 | 631 | 509 | 70.5 | 32.1 | 81.5 |
| | Min | 0.60 | 3.0 | 0.60 | 39.6 | 0.70 | 0.70 | 0.70 | 0.70 |
| | Max | 9044 | 3615 | 392 | 2696 | 2015 | 144 | 95.3 | 225 |
| | CV/% | 178 | 159 | 196 | 122 | 153 | 60.1 | 129 | 64.8 |
| | OSR/% | 20.0 | 0 | 5.80 | 77.1 | 0 | 0 | 8.60 | 45.7 |
| Reference value* | | 2500 | 4200 | 172 | 140 | 36000 | 2000 | 82.0 | 61.0 |

* Risk intervention values (GB 36600—2018) and the superfund soil screening guidance of the United States; CV: Coefficient of variation; OSR: Over-standard rate

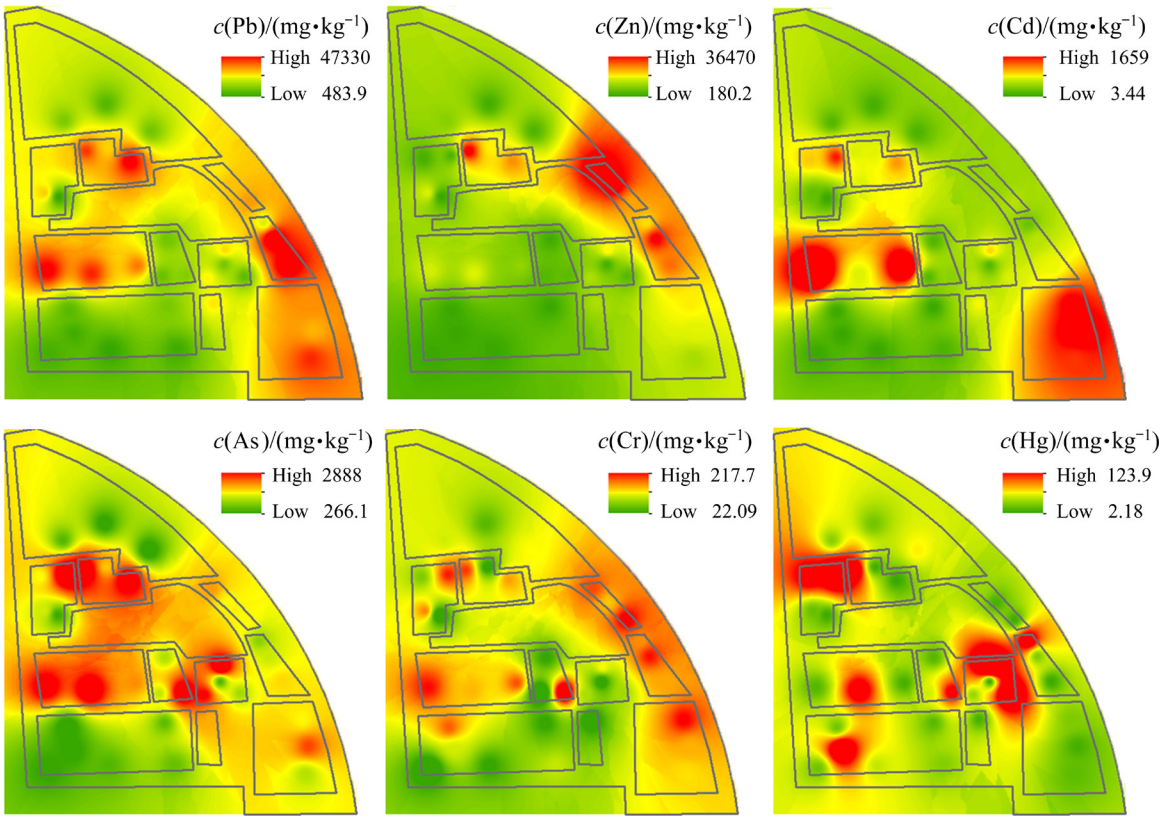


**Fig. 2** Horizontal distribution of heavy metals in surface soil

within the soils at the site (Table 1), there overall horizontal distribution patterns were generally consistent. The hotspots of Pb and Cd were distributed in warehouses and raw material yards, while As was distributed more widely, and even covered the whole smelter. From the preliminary site survey it was found that there were no complete covering barriers in these areas and apparent contamination leaks occurred. Refining and processing procedures are associated with the generation of fine particles containing heavy metals [25], which is a vital source of heavy metal exposure for soil. In addition, the remaining slags and raw material were treated randomly. The residual heavy metals could migrate into the soil due to rainwater leaching, natural weathering and microbial activities [15]. Previous studies have found that harmful leached components (As, Cd and Pb) in the Pb/Zn smelting slags were considerably high, which could release and increase the content of heavy metals in soil [26]. Cd and As were recognized as guest elements in raw ores which were released synchronously during the refining and processing [27]. Thus, a similar spatial distribution pattern may result in the same polluted origin and pathway. The high content of Hg was concentrated in the furnace area and the raw material yard. Coal was recognized as remarkable sources of Hg [28], and the storage and combustion of coal might explain the higher Hg level in the soil. Moreover, Hg could be released into the global pool during high temperature processes, while only part of it is deposited in local soils [29]. Obvious hotspots of high Cr were observed in slag dumps. It was consistent with previous results that Cr was enriched in smelting slags due to its refractory features [30]. Meanwhile, there were no obvious pollution sources in non-productive areas (east of the site), but high heavy metal levels occurred. Topography has been found to influence soil heavy metal migration due to differences in terrain, such as elevation and slope [31]. The smelter had a relatively lower elevation in the east, resulting in soil movement due to runoff erosion and easily causing the enrichment of soil heavy metals in the east [10]. Overall, the accumulation patterns of dominant pollutants represented the legacy of former intensive producing activities and topography slope.

Statistical results exhibited that the contents of Pb, Cd, As, Cr and Hg in soil core still exceeded the reference value in different degrees (Table 1). The downward transport of multiple heavy metals led to severe comprehensive pollution. The vertical distribution of the six pollutants in the soil cores of the site is illustrated in boxplots (Fig. 3). From the

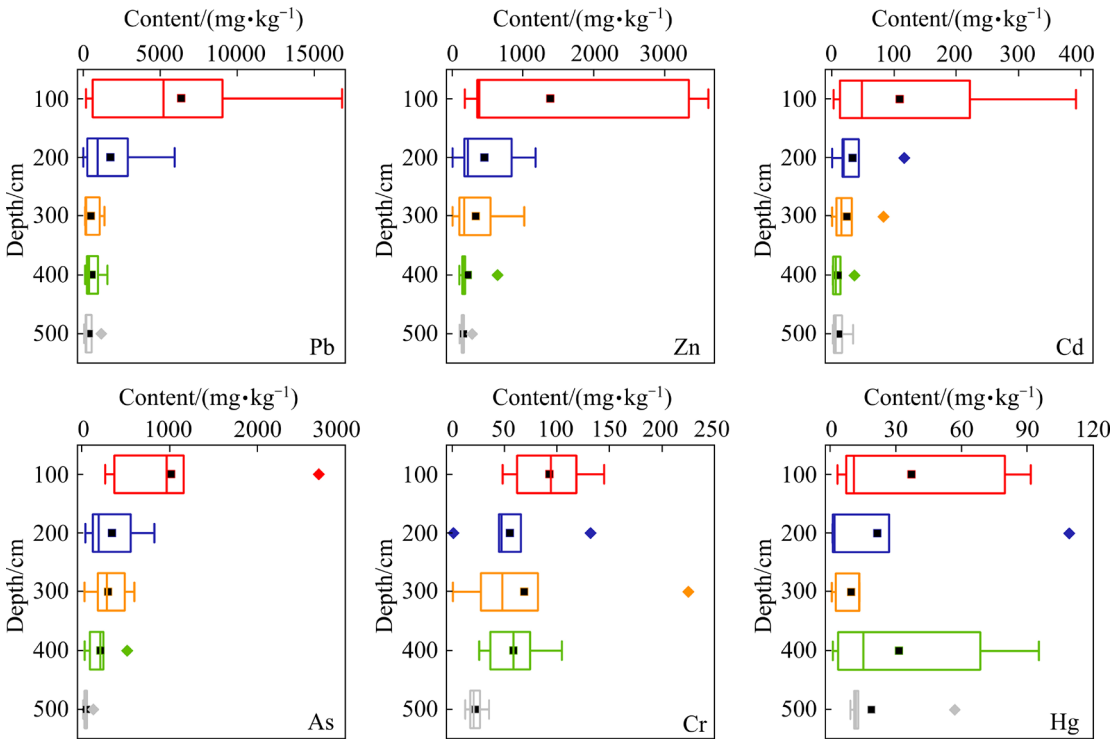


**Fig. 3** Vertical distribution of heavy metals

perspective of the whole site, the content of heavy metals decreased gradually with the increase of depth, as described by XU et al [4]. However, vertical distribution of heavy metals did not show regular change trend along the depth for a specific soil core. Similar vertical distribution patterns were found in previous studies [2]. The field records showed that the layer was almost entirely backfilled soils with complex properties from top to base. Thus, the diversity of soil interception might result in the complex vertical distribution of heavy metals [10]. The pollution depth of heavy metals reached 400 cm, indicating that some heavy metals in the top soil had been leached into deeper layers. Long-term leaching, natural weathering and microbial activities could mobilize heavy metals to migrate downward [15], which might lead to the accumulation of heavy metal in deeper layers. Meanwhile, it is worth noting that the average content of As still exceeded the risk intervention values (GB 36600 — 2018) even at 400 cm (212 mg/kg). Table S3 of SD showed that the pH values of soils were alkalescent. MASSCHELEYN et al [32] believed that As was released into soil solution in a weakly alkaline environment. High leaching enhanced the migration capacity of As in the profile which ultimately accumulated in the deep soil. The average content of Pb decreased considerably at 200 cm (1886 mg/kg compared to 6542 mg/kg at 100 cm), indicating that Pb was more immobile than As. This phenomenon might be directly related to the mineralogical composition of Pb fractions, and relatively insoluble phases ($PbSO_4$, $PbSO_4$·PbO and PbS) usually existed in the smelting soils [25]. In addition, the fate of heavy metals was further complicated by the dynamic changes of soil components and their interactions [33,34]. More in-depth investigations were warranted, especially on their immobilization mechanism and contribution to heavy metals in the fickle interface.

### 3.3 Correlations analysis among heavy metals

Internal relationship analysis of heavy metals was performed to imply their possible sources and pathways [1]. As shown in Fig. 4, a remarkably positive correlation at $P < 0.05$ was exhibited between the elemental pairs, Pb−Zn (0.69), As−Pb (0.61), As−Cd (0.59), and Cr−Pb (0.57), indicating compounding pollution relationship or homologous relationship among these heavy metals. Hg was not significantly correlated to the most of the other heavy metals considered, which meant that their concentration changes were not similar and Hg might share an individual origin. Spatial distribution showed that Hg was concentrated in the furnace area and raw material yard (Fig. 2), and coal could be the primary source of Hg except for smelting activities [28]. Thus, the complicated sources of soil Hg contributed to the unique spatial distribution and internal relationship. In addition, the high correlation coefficients among most of the heavy metals suggested that their formation and migration paths might be consistent [4] due to multi-heavy metal interactions intensified by long-term intensive production [2].

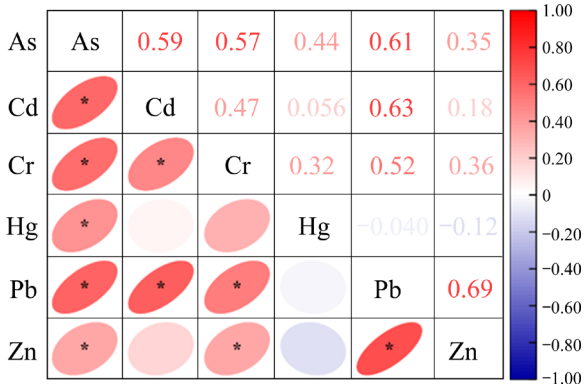


**Fig. 4** Correlation plot among heavy metals (∗ $P$<0.05 significance level)

### 3.4 Provenance and contribution of heavy metal pollution

The significant positive correlation in heavy metals provided a prerequisite for tracing heavy metal sources by lead isotope [9]. The related Pb isotope values ($^{208}Pb/^{206}Pb$ and $^{206}Pb/^{207}Pb$) of smelting ores, coals and vehicle exhaust were derived from the literature (Table S4 of SD), which might be potential heavy metal endmembers [13]. Figure 5(a) presents Pb isotopic composition of soil from the abandoned Pb smelting site. Background soils ($n$=3) displayed average Pb isotope ratios of 1.1927 ($^{206}Pb/^{207}Pb$) and 2.0797 ($^{208}Pb/^{206}Pb$), respectively. The composition was comparable to what was previously found in deep soils for Baiyin [9] and Guilin [18], which could represent the natural background value for the study area (geological source). $^{206}Pb/^{207}Pb$ and $^{208}Pb/^{206}Pb$ isotope ratios for contaminated soils varied from 1.1356 to 1.1738

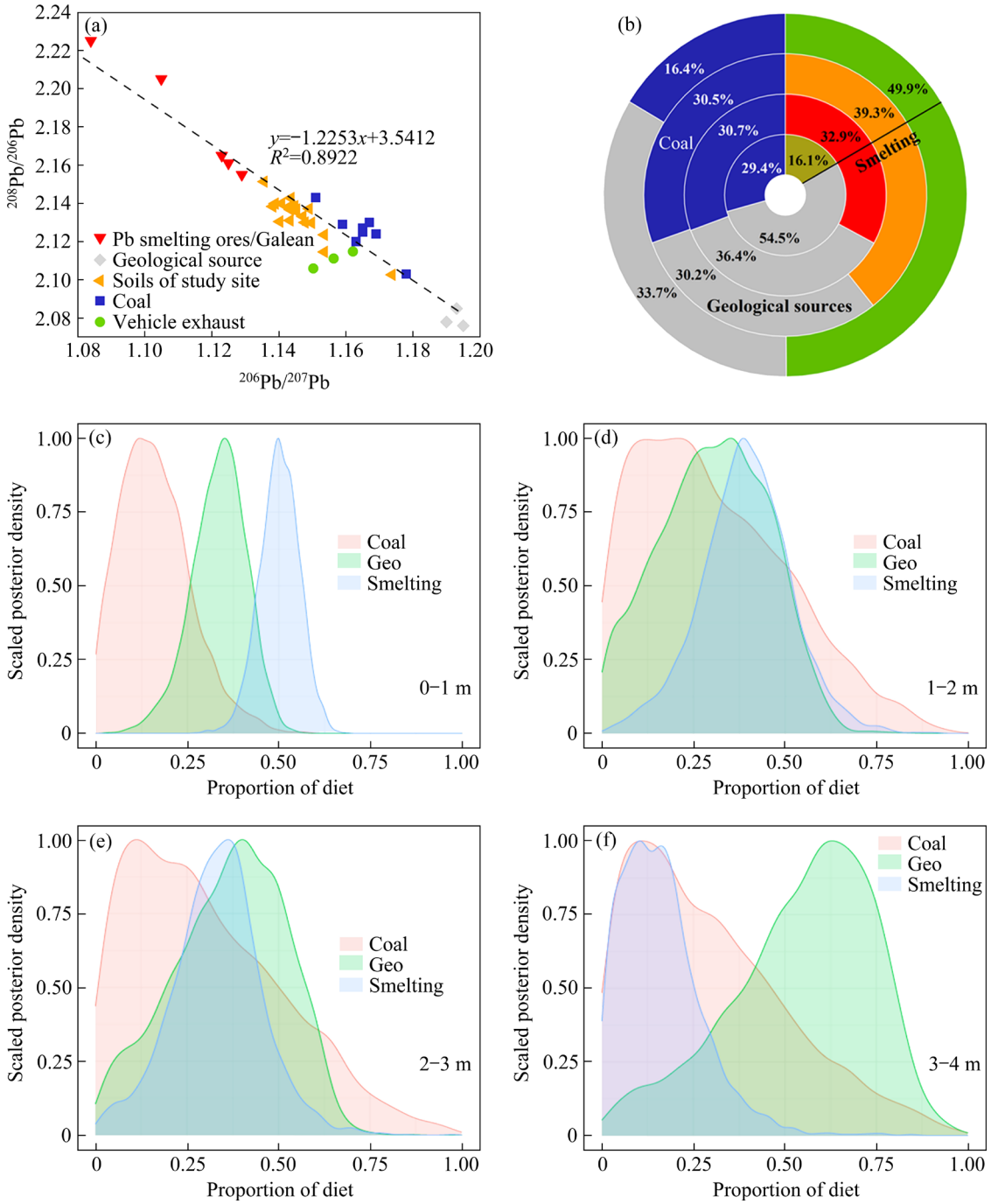


**Fig. 5** Diagram of $^{206}Pb/^{207}Pb$ vs $^{208}Pb/^{206}Pb$ in soils (a), relative contribution of endmembers (b) and scaled posterior density resolved by MixSIAR model (c−f)

and from 2.1026 to 2.1513. The large variation range of Pb isotope composition of soil indicated complex sources. The characteristics of $^{206}Pb/^{207}Pb$ and $^{208}Pb/^{206}Pb$ in contaminated soil were markedly lower and higher than those of deep soils, respectively. This agreed with respective Pb isotope values in previous findings that anthropogenic Pb sources have higher $^{208}Pb/^{206}Pb$ and lower $^{206}Pb/^{207}Pb$ as compared to geogenic Pb [9,13,17]. Soil cores also displayed different depth trends concerning their Pb isotopic composition. Specifically, $^{206}Pb/^{207}Pb$ increased from 1.1428 to 1.1738 with the depth. The Pb isotopic composition for deeper soils was far from the smelting ore and closer to the naturally occurring than topsoil. The results indicated that anthropogenic activities made limited contributions to heavy metals in deep soil, which was consistent with the vertical distribution

pattern of low concentration in deep soil (Fig. 3). Pb isotopic composition fitting analysis confirmed that smelting ores/Galena, coal and geological source all define a common linear trend, covering the sample populations for contaminated soils ($R^2$=0.8922). However, Pb isotope ratios for vehicle exhaust ($^{206}Pb/^{207}Pb$: 1.1503−1.1621 and $^{208}Pb/^{206}Pb$: 2.1059−2.1148) [18] deviated from this linear trend. This suggests that a mixing line exists between Pb from the smelting activities and geological sources, whereas the contribution from traffic sources, respectively vehicle exhaust, appears to be negligible. In contrast, the contribution from coal consumption cannot be ruled out, as they are normally used as the fuel or reducing agent in metallurgical processes, which could be a direct source of contaminants such as As, and Hg [35]. Thus, large spatial variation in the Pb isotopic compositions of smelting soils could be explained using different mixing proportions for the different endmembers.

To further quantify the contribution of each endmember to Pb by the $^{206}Pb/^{207}Pb$ and $^{208}Pb/^{206}Pb$ in contaminated soils, the MixSIAR model was used. The discrimination values were set to be zero for $^{206}Pb/^{207}Pb$ and $^{208}Pb/^{206}Pb$ because of their relatively high resistance against isotope fractionation during severe industrial processes [9]. The average Pb isotopic compositions of smelting ores and galena were 1.1132 ($^{206}Pb/^{207}Pb$) and 2.1822 ($^{208}Pb/^{206}Pb$), respectively [36], which were considered as smelting sources in this study. Values for coal were taken from BI et al [37]. With considering the uncertainty of the provenance contribution, the scaled posterior density of the endmembers was resolved by MixSIAR model (Figs. 5(c−f)). The mean contribution from different sources to the Pb budget in the soils was illustrated in Fig. 5(b). Judged from the density distribution, smelting source contributes most of the anthropogenic Pb in topsoil, accounting for 49.9% on average. And 16.7% and 33.7% of Pb was supplied by coal combustion and geological source, respectively. As the depth increased, the contribution of anthropogenic activities decreased significantly, and geological sources were the main sources of heavy metals (Figs. 5(c−f)). Naturally occurring contributed 54.5% of the total Pb burden of in soil core on average (4.0 m, Figs. 5(b)). As discussed in Section 3.1, the concentrations of several metal(loid)s (Zn, Cd, As and Cr) and Pb in topsoil samples had a significant positive correlation, revealing that this metal(loid)s originated from the same pollution source. Therefore, the sources of soil Pb and other metal(loid)s highly correlated with Pb could be identified.

### 3.5 Pollution risk assessment based on MixSIAR−Monte Carlo model

By using Monte Carlo simulation, the concentration-oriented probability distribution of ecological risk index factor at different risk levels for each metal is presented in Table S5 of SD. The simulated mean $E_r^i$ of Cr (3.58), Hg (17.9) and Zn (2.60) were all far below the moderate risk threshold ($E_r$=40). Moreover, judged from the probability distribution, values were concentrated at a low level, which indicated these heavy metals present low ecological risks. The $E_r^i$ value of Pb spanned three levels (from low level to considerable level), with a mean risk factor of 38.5, very close to the moderate risk threshold, indicating a low ecological risk level. However, the probability of low risk and moderate risk were 55.4% and 36.3%, respectively, making it difficult to determine which risk level Pb belonged to. Relatively high risks of As (mean $E_r^i$=100) and Cd (mean $E_r^i$=93.2) in the entire region were observed, exceeding the considerable risk threshold ($E_r$=80). Furthermore, from the perspective of probability distribution, the ecological risk index factor of both As and Cd spanned five levels, indicating that the risk level of the study area was varied and there were high and very high risk probabilities. The basic trend of mean $E_r^i$ values in the smelting site was As > Cd > Pb > Hg > Hg > Zn. The histogram (Fig. S1 of SD) showed the distribution of ecological hazard index (RI) after 50000 random simulations, and the output fitting result conformed to the lognormal distribution. The predicted mean value of RI was 249, which was within the range of moderate risk. According to probability distribution, the predicted RI value ranged from 14.4 to 970 and was basically consistent with the distribution of the fitting results. The probabilities of low, moderate, considerable and high RI were 26.5%, 50.4%, 18.9% and 4.2%, respectively, and the probability of moderate ecological hazard index was dominant.

To directly recognize the impact of different heavy metals on ecological risk in the study site,

the influence degree of each heavy metal was calculated when assessing the overall ecological risk based on the sensitivity analyses module (Fig. S1 of SD). The contribution of each heavy metal to the ecological harm index was different. Cd elements ($T_r$=30) were the most sensitive elements affecting potential ecological risks, accounting for 47.7%, followed by As elements ($T_r$=10), which had a sensitivity of 39.6%. Previous studies have shown that ecological risks are closely related to the toxic-response factors of target heavy metals [22]. The Pb ($T_r$=5) concentration in the soil contributed 8.8% to overall ecological risk, despite its high concentration. For Hg elements ($T_r$=40), the result was reversed, with a contribution of 3.8% at relatively low concentrations in the whole site (Table 1, Fig. 2). ZHANG et al [38] showed that Hg elements have similar effects on potential ecological risks. The results indicated that heavy metals with a high toxic response and severe pollution have the greatest impact on the potential ecological risk [19]. Thus, Cd, As, Pb and Hg were identified as the primary pollution factors. It is necessary to strengthen the monitoring of these sensitive factors and pay special attention to their pollution situation in the subsequent remediation of the site. To differentiate the potential ecological risk caused by different pollution sources, a source-oriented risk evaluation model was established based on MixSIAR model. The cumulative probability distribution of the potential ecological risk of different sources is shown in Fig. 6. The mean RI values attributed to smelting activities, coal and geological sources were 114, 54 and 77, respectively. Obviously, the risk values of all sources were below the moderate risk threshold (RI=150). For specific sources, heavy metals from coals and geological sources might not adversely affect the ecological risk due to more than 90th percentile (96.1% and 92.6%, respectively) of RI value were below 150 (Fig. 6, Table S6 of SD). The ecological risk from smelting activities occupied 15.8% at a moderate risk level and had a more significant contribution to RI value than other sources, which could not be ignored. Multiple potential smelting sources still existed in the site, including remaining slags and raw materials, etc. Considering the uncontrollability of the natural sources, the control of these sensitive pollutants and the disposal of potential smelting sources should be in priority. In the present study, the concentration randomness caused by spatial variation of heavy metals was converted to probability distribution. The sensitive factors were identified and the contributions of endmembers to risks were apportioned. The integrated analysis reduced the uncertainty for the more reliable estimation of ecological risks.

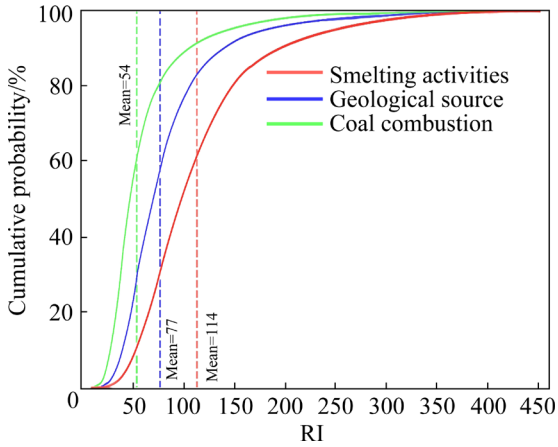


**Fig. 6** Cumulative probability distribution of potential ecological risk caused by different endmembers

## 4 Conclusions

(1) Soils were seriously contaminated, with Pb, Zn, As, Cd, Cr and Hg being the dominant pollutants. Significant spatial heterogeneities of heavy metals were observed, which represented the legacy of former producing activities and topography slope. The pollution depth of heavy metals reached 400 cm, which might be attributed to long-term leaching. Soil properties and chemical speciation of heavy metals also affected the downward migration of heavy metals.

(2) Pb isotopic signature of smelting, coal and geological source defined a common linear trend covering the sample populations for contaminated soils. The scaled posterior densities of the endmembers were resolved by MixSIAR model and indicated smelting activities contributed 49.9% of the heavy metals in topsoil on average, while 16.4% and 33.7% originated from coal combustion and geological source, respectively. The Pb isotopic composition for deeper soils was far from the smelting ore and closer to the naturally occurring than topsoil.

(3) Concentration randomness was solved by a probabilistic approach. Monte Carlo simulation

outputs showed RI conformed to the lognormal distribution and the moderate risk level was dominant. Cd, As, Pb and Hg contributed 47.7%, 39.6%, 8.8% and 3.8% of the sensitivity to ecological risks, respectively. Source-oriented probabilistic risk evaluation determined smelting activities as the most significant contributor to ecological risk. The control of Cd, As, Pb and Hg and the proper disposal of potential smelting sources should be in priority.

## Acknowledgments

The research was funded by the National Key Research and Development Program of China (No. 2019YFC1803601), the National Natural Science Foundation of China (No. 42177392) and the Fundamental Research Funds for the Central Universities of Central South University, China (No. 2021zzts0122).

## Supplementary data

Supplementary data in this paper can be found at: http://tnmsc.csu.edu.cn/download/25-p3222-2022-0585-Supplementary_Data.pdf.

## References

[1] ZENG Jia-qing, LUO Xing-hua, CHENG Yi-zhi, KE Wen-shun, HARTLEY W, LI Chu-xuan, JIANG Jun, ZHU Feng, XUE Sheng-guo. Spatial distribution of toxic metal(loid)s at an abandoned zinc smelting site, Southern China [J]. Journal of Hazardous Materials, 2022, 425: 127970.

[2] LI Shu-zhen, ZHAO Bi, JIN Ming, HU Liang, ZHONG Hui, HE Zhi-guo. A comprehensive survey on the horizontal and vertical distribution of heavy metals and microorganisms in soils of a Pb/Zn smelter [J]. Journal of Hazardous Materials, 2020, 400: 123255.

[3] WU Yao-guo, XU You-ning, ZHANG Jiang-hua, HU Si-hai. Evaluation of ecological risk and primary empirical research on heavy metals in polluted soil over Xiaoqinling gold mining region, Shaanxi, China [J]. Transactions of Nonferrous Metals Society of China, 2010, 20: 688−694.

[4] XU Lei, DAI Hui-ping, SKUZA L D, WEI Shu-he. Comprehensive exploration of heavy metal contamination and risk assessment at two common smelter sites [J]. Chemosphere, 2021, 285: 131350.

[5] QIAN Zi-yan, XUE Sheng-guo, CUI Meng-qian, WU Chuan, LI Wai-chin. Arsenic availability and transportation in soil−rice system affected by iron-modified biochar [J]. Journal of Central South University, 2021, 28(6): 1901−1918.

[6] KE Wen-shun, ZENG Jia-qing, ZHU Feng, LUO Xing-hua, FENG Jing-pei, HE Jin, XUE Sheng-guo. Geochemical partitioning and spatial distribution of heavy metals in soils contaminated by lead smelting [J]. Environmental Pollution, 2022, 307: 119486.

[7] ZENG Jia-qing, LI Chu-xuan, WANG Jin-ting, TANG Lu, WU Chuan, XUE Sheng-guo. Pollution simulation and remediation strategy of a zinc smelting site based on multi-source information [J]. Journal of Hazardous Materials, 2022, 433: 128774.

[8] YAN Hong-jie, ZHANG He-yang, SHI Ya-jun, ZHOU Ping, LI Huan, WU Dong-ling, LIU Liu. Simulation on release of heavy metals Cd and Pb in sediments [J]. Transactions of Nonferrous Metals Society of China, 2021, 31: 277−287.

[9] HE Bi-hong, ZHAO Xiao-lan, LI Ping, LIANG, Jian-jun, FAN Qiao-hui, MA Xiang-xian, ZHENG Guo-dong, QIU Jun-li. Lead isotopic fingerprinting as a tracer to identify the pollution sources of heavy metals in the southeastern zone of Baiyin, China [J]. Science of the Total Environment, 2019, 660: 348−357.

[10] YANG Xue, YANG Yong, WAN Yong-yong, WU Ruo-jing, FENG De-kun, LI Ke. Source identification and comprehensive apportionment of the accumulation of soil heavy metals by integrating pollution landscapes, pathways, and receptors [J]. Science of the Total Environment, 2021, 786: 147436.

[11] SHEN Feng, LIAO Ren-mei, ALI A, MAHAR A, GUO Di, LI Rong-hua, SUN Xi-ning, AWASTHI M K, WANG Quan, ZHANG Zeng-qiang. Spatial distribution and risk assessment of heavy metals in soil near a Pb/Zn smelter in Feng County, China [J]. Ecotoxicology and Environmental Safety, 2017, 139: 254−262.

[12] JIANG Zhi-chao, GUO Zhao-hui, PENG Chi, LIU Xu, ZHOU Zi-ruo, XIAO Xi-yuan. Heavy metals in soils around non-ferrous smelteries in China: Status, health risks and control measures [J]. Environmental Pollution, 2021, 282: 117038.

[13] WANG Peng-cong, LI Zhong-gen, LIU Jin-ling, BI Xiang-yang, NING Yong-qiang, YANG Shao-chen, YANG Xiao-jing. Apportionment of sources of heavy metals to agricultural soils using isotope fingerprints and multivariate statistical analyses [J]. Environmental Pollution, 2019, 249: 208−216.

[14] CUI Xiao-wei, GENG Yong, SUN Rui-rui, XIE Mei, FENG Xiu-wei, LI Xin-xin, CUI Zhao-jie. Distribution, speciation and ecological risk assessment of heavy metals in Jinan Iron & Steel Group soils from China [J]. Journal of Cleaner Production, 2021, 295: 126504.

[15] LUO Xing-hua, WU Chuan, LIN Yong-cheng, LI Wai-chin, DENG Min, TAN Jing-qiang, XUE Sheng-guo. Soil heavy metal pollution from Pb/Zn smelting regions in China and the remediation potential of biomineralization [J]. Journal of Environmental Sciences, 2023, 125: 662−677.

[16] XIA Ya-fei, GAO Ting, LIU Yu-hui, WANG Zhong-gen, LIU Cheng-shuai, WU Qi-qi, QI Meng, LV Yi-wen, LI Fang-bai. Zinc isotope revealing zinc's sources and transport processes in karst region [J]. Science of the Total Environment, 2020, 724: 138191.

[17] LIANG Xing-yu, WANG Chuan, SONG Zheng-cheng, YANG Shao-chen, BI Xiang-yang, LI Zhong-gen, LI Ping. Soil metal(loid)s pollution around a lead/zinc smelter and source apportionment using isotope fingerprints and receptor

models [J]. Applied Geochemistry, 2021, 135: 105118.

[18] KONG Jing, GUO Qing-jun, WEI Rong-fei, STRAUSS H, ZHU Guang-xu, LI Si-liang, SONG Zhao-liang, CHEN Tong-bin, SONG Bo, ZHOU Ting, ZHENG Guo-di. Contamination of heavy metals and isotopic tracing of Pb in surface and profile soils in a polluted farmland from a typical karst area in southern China [J]. Science of the Total Environment, 2018, 637/638: 1035−1045.

[19] HUANG Jing-ling, WU Yu-ying, SUN Jia-xun, LI Xiao, GENG Xiao-lei, ZHAO Meng-lu, SUN Ting, FAN Zheng-qiu. Health risk assessment of heavy metal(loid)s in park soils of the largest megacity in China by using Monte Carlo simulation coupled with Positive matrix factorization model [J]. Journal of Hazardous Materials, 2021, 415: 125629.

[20] CHEN Han-rui, WANG Lu, HU Bi-feng, XU Jian-ming, LIU Xing-mei. Potential driving forces and probabilistic health risks of heavy metal accumulation in the soils from an e-waste area, southeast China [J]. Chemosphere, 2022, 289: 133182.

[21] TONG Rui-peng, YANG Xiao-yi, SU Han-rui, PAN Yue, ZHANG Qiu-zhuo, WANG Juan, LONG Ming-ce. Levels, sources and probabilistic health risks of polycyclic aromatic hydrocarbons in the agricultural soils from sites neighboring suburban industries in Shanghai [J]. Science of the Total Environment, 2018, 616/617: 1365−1373.

[22] GU Xiang, WANG Zong-xing, WANG Jing, OUYANG Wei, WANG Bao-dong, XIN Ming, LIAN Mao-shan, LU Shuang, LIN Chun-ye, HE Meng-chang, LIU Xi-tao. Sources, trophodynamics, contamination and risk assessment of toxic metals in a coastal ecosystem by using a receptor model and Monte Carlo simulation [J]. Journal of Hazardous Materials, 2022, 424: 127482.

[23] YAO Wen-bin, HUANG Lei, YANG Zhi-hui, ZHAO Fei-ping. Effects of organic acids on heavy metal release or immobilization in contaminated soil [J]. Transactions of Nonferrous Metals Society of China, 2022, 32: 1277−1289.

[24] HE Song, LI Pei-yue, SU Feng-mei, WANG Dan, REN Xiao-fei. Identification and apportionment of shallow groundwater nitrate pollution in Weining Plain, northwest China, using hydrochemical indices, nitrate stable isotopes, and the new Bayesian stable isotope mixing model (MixSIAR) [J]. Environmental Pollution, 2022, 298: 118852.

[25] ETTLER V. Soil contamination near non-ferrous metal smelters: A review [J]. Applied Geochemistry, 2016, 64: 56−74.

[26] SOBANSKA S, DENEELE D, BARBILLAT J, LEDÉSERT B. Natural weathering of slags from primary Pb−Zn smelting as evidenced by Raman microspectroscopy [J]. Applied Geochemistry, 2016, 64: 107−117.

[27] ZHONG Xi, CHEN Zi-wu, LI Ya-ying, DING Keng-bo, LIU Wen-shen, LIU Ye, YUAN Yong-qiang, ZHANG Miao-yue, BAKER A J M, YANG Wen-jun, FEI Ying-heng, WANG Yu-jie, CHAO Yuan-qing, QIU Rong-liang. Factors influencing heavy metal availability and risk assessment of soils at typical metal mines in Eastern China [J]. Journal of Hazardous Materials, 2020, 400: 123289.

[28] UNEP. Global Mercury Assessment [R]. Geneva: United Nations Environment Programme, 2018.

[29] PETALOTI C, TRIANTAFYLLOU A, KOUIMTZIS T, SAMARA C. Heavy metals in atmospheric particulate matter over a coal burning power production area of western Macedonia, Greece [J]. Chemosphere, 2006, 65: 2233−2243.

[30] BOHDAN K A, VLADIMÍR M, FRANTIŠEK V, IMASIKU N. Discrimination of lithogenic and anthropogenic sources of metals and sulphur in soils of the central-northern part of the Zambian Copperbelt Mining District: A topsoil vs. subsurface soil concept [J]. Journal of Geochemical Exploration, 2010, 104: 69−86.

[31] DING Qian, CHENG Gong, WANG Yong, ZHUANG Da-fang. Effects of natural factors on the spatial distribution of heavy metals in soils surrounding mining regions [J]. Science of the Total Environment, 2017, 578: 577−585.

[32] MASSCHELEYN P H, DELAUNE R D, PATRICK JR W H. Effect of redox potential and pH on arsenic speciation and solubility in a contaminated soil [J]. Environmental Science & Technology, 1991, 25: 1414−1419.

[33] ZHOU Qi-xing, LIU Yu-xia, LI Tian, ZHAO Hua-zhang, ALESSI D S, LIU Wei-tao, KONHAUSER K O. Cadmium adsorption to clay-microbe aggregates: Implications for marine heavy metals cycling [J]. Geochimica et Cosmochimica Acta, 2020, 290: 124−136.

[34] ZENG Jia-qing, KE Wen-shun, DENG Min, TAN Jing-qiang, LI Chu-xuan, CHENG Yi-zhi, XUE Sheng-guo. A practical method for identifying key factors in the distribution and formation of heavy metal pollution at a smelting site [J]. Journal of Environmental Sciences, 2023, 127: 552−563.

[35] MUKHERJEE A B, ZEVENHOVEN R. Mercury in coal ash and its fate in the Indian subcontinent: A synoptic review [J]. Science of the Total Environment, 2006, 368: 384−392.

[36] XING Wei-qin, YANG Hao, IPPOLITO J A, ZHANG Yu-qing, SCHECKEL K G, LI Li-ping. Lead source and bioaccessibility in windowsill dusts within a Pb smelting-affected area [J]. Environmental Pollution, 2020, 266: 115110.

[37] BI Xiang-yang, LI Zhong-gen, WANG Shu-xiao, ZHANG Lei, XU Rui, LIU Jin-ling, YANG Hong-mei, GUO Ming-zhi. Lead isotopic compositions of selected coals, Pb/Zn ores and fuels in China and the application for source tracing [J]. Environmental Science & Technology, 2017, 51(22): 13502−13508.

[38] ZHANG Hai-wei, ZHANG Fei, SONG Jia, TAN M L, KUNG H T, JOHNSON V C. Pollutant source, ecological and human health risks assessment of heavy metals in soils from coal mining areas in Xinjiang, China [J]. Environmental Research, 2021, 202: 111702.

# 基于随机模拟的冶炼场地重金属污染及生态风险评价

罗兴华[1]，曾嘉庆[1]，吴 川[1]，邱坤艳[2]，李超然[2]，可文舜[1]，薛生国[1]

1. 中南大学 冶金与环境学院，长沙 410083；
2. 河南大学 纳米杂化材料应用技术国家地方联合工程研究中心，开封 475004

**摘 要：**选择某铅冶炼场地，采用地统计学和铅同位素示踪法分析重金属空间分布格局和污染来源，并基于不确定性理论的风险模型，系统评估场地重金属生态风险。结果表明，土壤铅、锌、砷、镉、铬和汞污染严重，空间异质性强。采用 MixSIAR 模型解构 3 个潜在源的铅同位素贡献密度分布，土壤重金属主要来自冶炼活动(49.9%)，燃煤(16.4%)和土壤母质(33.7%)。基于随机模拟的潜在生态风险指数(RI)表明，场地重金属处于中等生态风险；其中冶炼活动对 RI 累积贡献最大；镉、砷、铅和汞对 RI 的方差贡献最大，对场地的污染起主导作用。因此，应该优先关注场地土壤镉、砷、铅和汞污染的防控及潜在冶炼源的处置。

**关键词：**冶炼场地；重金属；铅同位素；随机模拟；生态风险

**(Edited by Bing YANG)**